The Low-Temperature Crystal Structure of the Pure-Spermine Form of Z-DNA Reveals Binding of a Spermine Molecule in the Minor Groove[†,‡]

Daniel Bancroft,[§] Loren Dean Williams,[∥] Alexander Rich,[*] and Martin Egli[*,⊥]

Department of Biology, Massachusetts Institute of Technology, Cambridge, Massachusetts 02139

Received June 24, 1993; Revised Manuscript Received November 8, 1993[⊗]

ABSTRACT: The X-ray crystal structure of the pure-spermine form of the left-handed Z-DNA duplex $[d(CGCGCG)]_2$ has been determined at a temperature of −110 °C. Whereas the previously described room temperature structure of the pure-spermine form showed only the presence of a single "interhelix" spermine molecule, mediating contacts between neighboring duplexes (Egli et al., 1991), a second "intrahelix" spermine molecule as well as two hydrated sodium ions were found in the structure determined at low temperature. This second spermine molecule binds primarily within the minor groove of two hexamer duplexes that are stacked in an end-to-end fashion in the crystal lattice. Thus, the intrahelix spermine molecule interacts with a single infinite helix. The spine of hydration observed in other structures of Z-DNA hexamers is partially replaced and partially displaced by the intrahelix spermine molecule. In Z-DNA, phosphate groups are relatively closely spaced across the minor groove compared to the right-handed double-helical conformation of B-DNA. The intrahelix spermine molecule decreases cross-groove electrostatic repulsion within the Z-DNA helix, thereby increasing its relative stability. This structure may therefore provide an explanation for the role of spermine as a very effective inducer of the conformational B-DNA to Z-DNA transition with alternating dG–dC sequences in solution.

We have recently reported the X-ray crystal structure of the pure-spermine form of Z-DNA, a complex between a left-handed DNA hexamer with sequence $[d(CGCGCG)]_2$ and the polyamine spermine, obtained from a spermine solution lacking magnesium or other multivalent cations (Egli et al., 1991). The conformation, orientation, and interactions of Z-DNA in the pure-spermine form crystal differ from those of other forms which are generally similar to each other. For example, the pure-sodium form of Z-DNA (Chevrier et al., 1986) displays nearly the same conformation, orientation, and interactions of the Z-DNA duplex as multivalent cationic forms (Wang et al., 1984; Ho et al., 1987; Gessner et al., 1989; Schneider et al., 1992), even when multivalent cations are supplemented with spermine (Wang et al., 1979). In comparison to other forms, the base pairs in the pure-spermine form duplex are shifted away from the minor groove into the convex surface by about 1 Å. In addition, the minor groove is narrower and the average helical rise per base pair is reduced by more than 0.1 Å compared to the multivalent cationic forms. Thus, a complete turn of the pure-spermine form Z-DNA helix (12 base pairs per turn) is around 2 Å shorter than a complete turn in other forms. The structure of the pure-spermine form indicated that Z-DNA has greater conformational freedom than previously assumed.

The X-ray intensity data of the original pure-spermine form of Z-DNA were collected at room temperature (RT). The Fourier electron density maps of that structure revealed one spermine molecule, here referred to as the "interhelix" spermine molecule. Infinite helices are formed in the lattice by end-to-end stacking of hexamer duplexes, where every sixth phosphate within the infinite helix is absent due to the lack of 5′-phosphate groups in the hexamers. The interhelix spermine molecule mediates the close approach of these infinite helices within the lattice by simultaneously binding to three stacks. It neutralizes repulsive phosphate interactions between helices and bridges them by a hydrogen-bonding network. This spermine molecule forms hydrogen bonds exclusively with convex surfaces (the Z-DNA equivalent of the major groove) of duplexes and with phosphate oxygens.

Apart from the single spermine molecule described above, it was not possible to assign cations unambiguously to other Fourier electron density peaks in the RT structure. Thus, the 10 negative charges of phosphate groups of the hexamer duplex were not neutralized by the four positive charges of the protonated amino and imino nitrogens of spermine in the final refined structure. To resolve ambiguities about cation interaction and conformation, we collected an additional data set at −110 °C. Decreasing the thermal motion within a crystal increased the fine detail of the electron density maps and has allowed us to determine aspects of conformation and interaction that were not discernible at room temperature.

Here we describe the three-dimensional structure of the pure-spermine form of Z-DNA refined from X-ray data collected at low temperature (LT). Inspection of the LT Fourier electron density maps revealed a second spermine molecule, unexpectedly bound in the narrow minor groove. This second spermine molecule, referred to here as the "intrahelix" spermine molecule, binds primarily to base functions at the floor of the minor groove and interacts with a single infinite helix. It binds to two hexamer duplexes that are stacked in the lattice, thereby further stabilizing the infinite helix. This spermine molecule partially replaces and partially

[†] This work was supported by grants from the National Institutes of Health, the American Cancer Society, the National Science Foundation, the Office of Naval Research, and the National Aeronautics and Space Administration. L.D.W. acknowledges support by the Medical Foundation, Boston, MA.

[‡] The atomic coordinates have been deposited with the Brookhaven Protein Data Bank (entry number 131D).

[*] Authors to whom correspondence should be addressed.

[§] Current address: Biochemistry Department, School of Medicine, University of Utah, Salt Lake City, UT 84132.

[∥] Current address: School of Chemistry and Biochemistry, Georgia Institute of Technology, Atlanta, GA 30332-400.

[⊥] Current address: Organic Chemistry Laboratory, ETH Swiss Federal Institute of Technology, CH-8092 Zürich, Switzerland.

[⊗] Abstract published in *Advance ACS Abstracts,* January 1, 1994.

0006-2960/94/0433-1073$04.50/0

displaces water molecules normally bridging cytosine O2 oxygens from opposite strands in the minor groove. In addition, the intrahelical spermine molecule contacts two phosphate oxygens at the surface of the minor groove, thereby relieving repulsive interactions between phosphates normally present at that site in the Z-DNA duplex.

It is well known that polyamines are critical components of biological systems and that, among other functions, they appear to mediate interactions of biological anions such as membranes and nucleic acids. High ionic strengths are required to promote the formation of the left-handed conformation *in vitro* (Pohl & Jovin, 1972). Even when cytosine is methylated at the 5-position, a sodium ion concentration of almost 1 M is needed to convert alternating dG–dC sequences from right-handed B-DNA to left-handed Z-DNA (Behe & Felsenfeld, 1981). In contrast, only low concentrations, similar to those found *in vivo*, of certain polyamines are required to induce the conformational B–Z transition in solution (e.g., Behe & Felsenfeld, 1981; Chen et al., 1984; Thomas & Messner, 1986; Basu et al., 1990; Rao et al., 1990; Thomas et al., 1991). Among those, spermine, which is the largest and most complex polyamine in eukaryotes (positive charge of four at pH 7), is a particularly effective inducer of the conformational transition. Parameters influencing the effects of polyamines on the B–Z transition are the total positive charge as well as the lengths of the alkyl chains separating the positively charged nitrogens. It has been shown that the central butyl group linking the imino nitrogens in spermine is of crucial importance in this respect (Basu & Marton, 1987; Vertino et al., 1987). Earlier X-ray crystallographic studies have provided evidence for a thermodynamic stabilization of Z-DNA through binding of spermine and related polyamines to phosphate groups and various sites on the convex surface (Wang et al., 1979; Tomita et al., 1989; Egli et al., 1991). The binding mode of spermine in the minor groove observed in the present crystal structure suggests a completely different role of spermine in the promotion and stabilization of left-handed Z-DNA. Rather than just interacting with readily accessible convex surface sites on the Z-DNA duplex, spermine may exert its effect by stabilizing left-handed segments through bridging closely spaced phosphate groups and cytosine O2 oxygens from opposite strands within the minor groove.

MATERIALS AND METHODS

DNA Synthesis and Purification. The self-complementary DNA hexamer d(CGCGCG) was synthesized, purified, and crystallized as previously described (Egli et al., 1991).

Data Collection and Reduction. A crystal with dimensions 0.35 × 0.30 × 0.30 mm was mounted at the end of a glass fiber with a small amount of silicone grease and flash-frozen (Hope, 1988) by immediate transfer into a −110 °C stream of nitrogen. Data were collected on a Rigaku AFC5R X-ray diffractometer equipped with a rotating copper anode and graphite monochromator ($\lambda_{Cu\,K\alpha}$ = 1.5406 Å). The space group is $P2_12_12_1$, and the unit cell constants, determined from 24 reflections with 2θ values between 11° and 25°, are a = 18.265 (4) Å, b = 30.69 (1) Å, and c = 42.46 (2) Å [V = 23 800 (20) Å^3]. A total of 14 081 reflections were collected by the ω scan method (scan speed 4°/min) to a resolution of 1 Å (2θ = 100°). Crystal decay was monitored with three reflections with 2θ values between 11° and 25°. The only observed decay was a 5% step decrease in the intensity of the standard reflections after 6580 reflections. This step decay resulted from formation of a small amount of frost on the crystal. The second portion of the data was therefore scaled by multiplying the intensities by a factor of 1.05. Data were corrected for Lorentz and polarization effects, and a semiempirical absorption correction based on the psi scan method was applied (North et al., 1968). The number of unique reflections observed above the $2\sigma(F_o)$ level was 9691.

Table 1: Selected Refinement Data

temperature	−110 °C
total number of unique reflections [$F_o > 2\sigma(F_o)$]	9575
R factor	18.0%
average $F_o - F_c$ discrepancy	8.26
RMS deviation of bonds from ideal	0.030 Å
RMS deviation of planes from ideal	0.022 Å
overdeterminacy ratio	7.2

		Resolution Breakdown			
		shell		sphere	
max resolution	no. of reflections[a]	$F_o - F_c$	R	$F_o - F_c$	R
5.00[b]	116 (117)				
3.00	430 (435)	15.7	0.098	15.7	0.098
2.50	383 (398)	14.2	0.144	15.0	0.115
2.00	828 (825)	12.3	0.162	13.6	0.132
1.70	1037 (1006)	9.6	0.164	12.1	0.141
1.50	1155 (1047)	8.2	0.180	10.9	0.148
1.20	2959 (2328)	7.0	0.225	9.2	0.167
1.00	2783 (2027)	5.9	0.256	8.3	0.180

[a] The numbers in parentheses refer to the number of reflections in the RT data set. [b] The 116 reflections between 5.0 and 20.0 Å were excluded from the refinement because they were heavily influenced by bulk solvent scattering.

Structure Solution and Refinement. The structure was isomorphous with that of the RT pure-spermine form, and the coordinates of the DNA and the single spermine molecule from that structure were used as the starting model. The DNA positions and isotropic temperature factors were refined using the Konnert–Hendrickson least-squares procedure (Hendrickson & Konnert, 1981) as modified for nucleic acids (Quigley et al., 1978) with relatively tight stereochemical restraints. Fourier electron sum ($2F_o - F_c$) and difference ($F_o - F_c$) density maps were calculated and displayed on an Evans and Sutherland PS390 graphics terminal with the program FRODO (Jones, 1982). In the electron density maps calculated after partial refinement, a continuous band of superimposed sum and difference density was observed in the minor groove and assigned to a second spermine molecule. The atoms of this spermine molecule were included in the subsequent refinement. Positions of water molecules were determined from additional sum and difference density maps. The two sodium ions were located by analyzing the coordination spheres of water molecules. Water molecules with contacts of less than 3 Å to at least six neighboring waters, spermine, or DNA atoms and roughly octahedral coordination geometry were then treated as sodium ions. For the final cycles, 9575 reflections between 5.0- and 1.0-Å resolution were included in the refinement. The R factor converged at 18.0% after the restraints were relaxed. In the final refined structure the asymmetric unit contained one DNA hexamer duplex (240 atoms), two spermine molecules, two sodium ions, and 62 water molecules. Table 1 lists selected refinement parameters. An example of the electron density maps surrounding the DNA and each spermine molecule is shown in Figure 1. The crystal structure was subsequently analyzed with the coordinates resulting from the KH-type restraint least-squares refinement.

In addition, the above coordinates were subjected to further refinement with program SHELXL-93 (Sheldrick, 1993). All 240 DNA atoms were treated anisotropically, and spermine

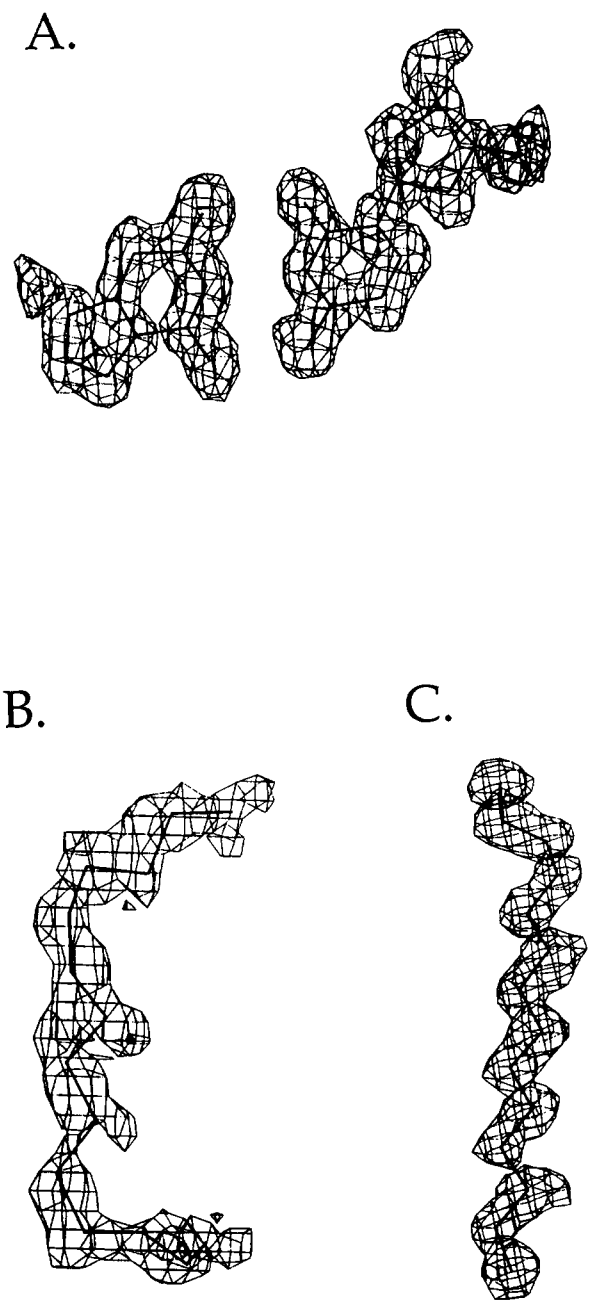

FIGURE 1: Sum electron density maps ($2F_o - F_c$) around (A) the terminal C(1)·G(12) base pair, (B) the intrahelix spermine molecule, and (C) the interhelix spermine molecule.

molecules and sodium ions as well as water molecules were refined isotropically. Soft restraints were applied for spermine molecules (bond lengths and 1–3 distances) and the two hydrated sodium ions (Na^+–O distances). Moreover, option DELU was used to compare and equilibrate Gaussian atomic displacement parameter (U_{ij}) components along the directions of chemical bonds. After 25 cycles of restraint conjugate gradient least-squares refinement, the R factor converged at 13.2% [9575 reflections with $F_o > 2\sigma(F_o)$, 2530 parameters]. The maximum shifts for coordinates and temperature factors were then smaller than 0.01 Å and 0.005 Å^2, respectively. Although only minor coordinate shifts for DNA atoms were observed, the geometry particularly of the intrahelical spermine molecule and consequently the electron density around it improved notably. Selected refinement parameters are listed in Table 2. Detailed protocols of the anisotropic refinement as well as listings of atomic coordinates, temperature factors, and bond lengths and angles are available from the authors upon request.

Table 2: Selected Anisotropic Refinement Data

total number of unique reflections [$F_o > 2\sigma(F_o)$]	9575
R factor	13.2%
overdeterminacy ratio	3.8

Resolution Breakdown

max resolution	no. of reflections	shell R	shell $K = \text{mean}(F_o)^2/\text{mean}(F_c)^2$
5.00	116		
2.37	963	0.113	1.045
1.91	937	0.123	1.068
1.66	975	0.115	1.121
1.50	951	0.130	1.090
1.38	941	0.139	1.049
1.29	976	0.141	1.072
1.21	943	0.156	1.101
1.14	969	0.157	1.050
1.07	925	0.168	1.076
1.00	995	0.201	1.147

RESULTS

DNA Conformation. In the pure-spermine form RT structure, the Z-DNA duplex was compressed along the helical axis compared to the magnesium and mixed spermine/magnesium forms. A full turn of the Z-DNA helix (12 base pairs) based on the average helical rise of the pure-spermine form was approximately 5% shorter than a complete turn based on the average rise of the mixed spermine/magnesium form. Furthermore, the bases in the pure-spermine form duplex were shifted toward the convex surface, and the minor groove was slightly narrower than in the other two forms. The differences between the geometries of the DNA in the pure-spermine form and in the magnesium and mixed spermine/magnesium forms have been analyzed in detail before (Egli et al., 1991). Here, we will therefore concentrate on the differences between the RT and LT structures of the pure-spermine form.

The change from RT to LT slightly alters the geometry of the pure-spermine form duplex. The average helical rise per base pair is 3.67 Å at RT and 3.61 Å at LT. Cooling thus increases the compression along the helical axis. At both temperatures the values for helical rise at CpG steps are slightly larger than those at GpC steps. The differences between these two types of helical rise are approximately 0.1 Å in the pure-spermine form and thus considerably smaller than those in the magnesium and mixed spermine/magnesium forms where the difference is approximately 0.5 Å.

The binding of a spermine molecule within the minor groove causes a shift of bases away from the groove and toward the convex surface. This is apparent from considerable offsets of the midpoints of the C6(pyrimidine)–C8(purine) lines of base pairs from the helical axis (x displacement). In the RT structure the average offset of base pairs is 3.8 (5) Å, and in the LT structure it is 4.0 (6) Å (the number in parentheses represents estimated standard deviation in least significant figure). Thus, cooling results in a slightly deeper minor groove and shifts the helical axis further away from the O2 positions of cytosines and into the minor groove. A comparison of the minor groove shapes of the LT pure-spermine and magnesium forms is shown in Figure 2. The deepening of the groove in the pure-spermine form upon binding of spermine is apparent from the longer distances between phosphate groups and the base pair.

In Z-DNA, the phosphate groups flanking the minor groove can be connected by two zig-zag lines. Phosphate groups of

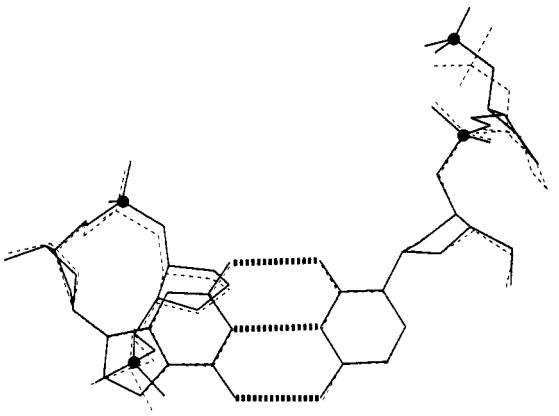

FIGURE 2: Comparison of the minor groove width of the LT pure-spermine form (solid lines) to the magnesium form (dashed lines), viewing along the helical axis. The C(1)·G(12) base pairs have been superimposed, and the other base pairs have been omitted. The phosphates and deoxyriboses of base pair G(2)·C(11) and the phosphates of base pair C(3)·G(10) have been included. Phosphorus atoms of the LT pure-spermine form are marked by black circles.

opposite strands are positioned such that the minor groove appears to alternately widen and contract when moving along the groove. This topology can be characterized by two types of distances, a long distance, representing the maximum width of the groove, and a short distance, representing the minimum width of the groove. In the hexamer duplex described here, the phosphorus atoms of one strand are numbered P2–P6, and those of the complementary strand are numbered P8–P12. The long distance is between P5 and P11, and the short distances are between P4 and P12 as well as between P6 and P10. In the LT structure of the pure spermine form, the long distance is 15.09 Å, and the short distances are 8.38 and 8.37 Å. In the RT structure, these distances were 15.08, 8.43, and 8.37 Å, and cooling therefore alters the groove width only minimally. In the magnesium form, the long distance is 16.05 Å and the short distances are 8.79 and 8.58 Å. In the mixed spermine/magnesium form, the long distance is 16.41 Å and the short distances are 8.64 and 8.88 Å. In Figure 2, the narrowing of the minor groove in the LT pure-spermine form compared to the magnesium form is visible from smaller cross-groove distances between phosphorus atoms.

The Z_I conformation of the backbone, where the phosphate groups are directed away from the convex surface, is more commonly observed in Z-DNA crystal structures than the Z_{II} conformation, where the phosphate groups are pointing toward the convex surface (Wang et al., 1981). The Z_I and Z_{II} conformations are distinguishable mainly by differences in the torsion angles ϵ and ζ and to a lesser degree by differences in α and β. The switch from Z_I to Z_{II} is accomplished without altering the position of the flanking deoxyriboses or the attached bases.

The backbone of the RT pure-spermine form duplex displayed Z_I/Z_{II} disorder in the region of the phosphate group of residue C(9) (Egli et al., 1991). At RT, both sum and difference electron density indicated that the Z_I conformation is predominant at this site but that the Z_{II} conformation is also partially occupied. In the LT structure the Z_I/Z_{II} disorder is also apparent in the region of the phosphate group of residue C(5). In this case the Z_I conformation also predominates over the Z_{II} conformation, and both sites were refined as Z_I (occupancy 1). The observation of Z_I/Z_{II} disorder in the pure-spermine form is consistent with the observation of Z_I/Z_{II} disorder in the recent LT structure of the magnesium form (Chen & Quigley, 1992). The polymorphic nature of the backbone in the crystalline state suggests that there may be an equilibrium between the Z_I and Z_{II} confomations in solution as well.

Spermine Conformations. The bond angles of the intrahelix spermine molecule vary between 107° and 123°, and the bond lengths vary between 1.45 and 1.58 Å (Figure 3A). For the interhelix spermine molecule, both the bond angles and bond lengths vary slightly less (between 104° and 115°, and between 1.51 and 1.62 Å, respectively). Bond lengths and angles of the two spermine molecules are shown in Figure 3. Bonds proximal to the nitrogen atoms tend to be shorter than bonds distal to the nitrogens. The small-molecule crystal structure of spermine phosphate hexahydrate (Iitaka & Huse, 1965) is an accurate geometrical standard to which the two spermine molecules observed here can be compared. In that structure, bond angles range from 109° to 112°, and bond lengths range from 1.49 to 1.54 Å, and C–N bond lengths are 1.50 Å on average.

The conformations of the interhelix spermine molecule and the intrahelix spermine molecule differ considerably, reflecting their dissimilar chemical environments. Their conformations are depicted in Figure 1B,C. The conformation of the interhelix spermine molecule is almost extended, and, with one exception, torsion angles are *antiperiplanar* (*ap*). This exception is the torsion angle around the C3–C4 bond, which lies in the negative *synclinal* (*-sc*) range. The conformation of this spermine molecule thus differs slightly from that observed in the RT structure. In the RT structure the C3–C4 torsion angle was also *-sc*, but the C11–C12 torsion angle at the opposite end of the molecule was negative *anticlinal* (*-ac*), resulting in bends at both ends. The conformational change upon cooling shifts N14 of this spermine closer to O6 of residue G(10) and away from N7 of the same residue (see Table 3 and the section on DNA–spermine interactions below).

The central region of the intrahelix spermine molecule, between the imino nitrogens N5 and N10, adopts an almost extended conformation, with the torsion angles around bonds C8–C9 and C9–N10 falling into the *-ac* range. This portion of the molecule runs along the floor of the minor groove. The torsion angles around bonds C4–N5 and N10–C11 are *+sc*, and both ends of the intrahelix spermine molecule bend away from the floor of the minor groove to contact the backbone via the terminal amino groups.

Interhelix Spermine–DNA Interactions. At RT and LT each interhelix spermine molecule interacts with three Z-DNA duplexes in the crystal lattice. The detailed interactions of the interhelix spermine molecule at RT have been described previously (Egli et al., 1991). In that structure, the interhelix spermine formed a total of nine hydrogen bonds to phosphate oxygens, base atoms, and water molecules. In the LT structure, these interactions are found as well, but with slightly altered geometry. Hydrogen-bonding distances between the interhelix spermine molecule and DNA and water molecules are listed in Table 3, and a schematic diagram of the binding of this spermine along the convex surface of one duplex is shown in Figure 6B. The only interactions in addition to those already observed at RT are the ones between amino nitrogen N14 of this spermine and the water molecules (18)W10 and (18)-W11. As described above, the most significant positional shifts are also found at this terminus of the interhelix spermine molecule. At RT spermine N14 is located 3.03 Å from O6 of residue G(10) and 3.00 Å from N7 of the same base. At LT this spermine nitrogen is shifted closer to O6 and away from N7. Together with the hydrogen bonds to the two newly revealed water molecules at LT, N14 is thus involved in three

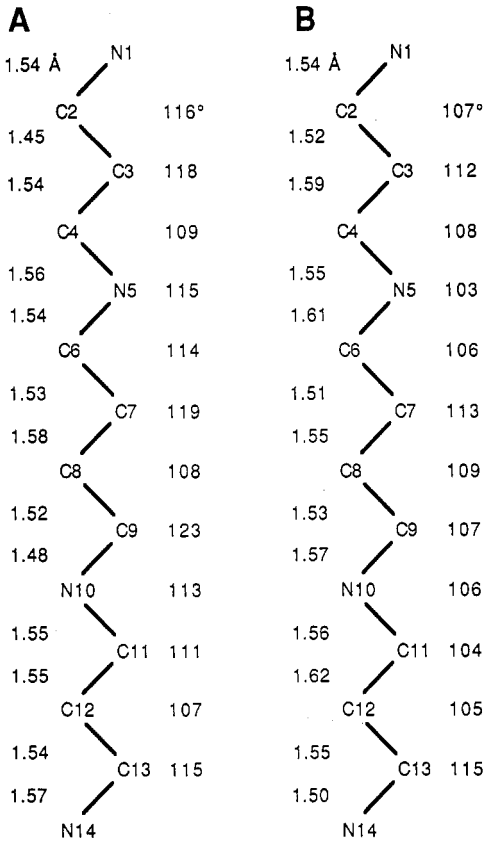

FIGURE 3: Geometry of the (A) intrahelix spermine molecule and (B) the interhelix spermine molecule. Bond lengths are on the left and bond angles are on the right.

Table 3: Hydrogen-Bonding Interactions of the Interhelix Spermine Molecule[a]

spermine	DNA/water		
atom (residue 13)	residue	atom	distance (Å)
N1	C(3)	O2P	2.73
N1	G(12)	O2P*	2.85
N1	15	W03	2.82
N5	C(11)	O1P*	2.80
N5	15	W01	2.86
N10	G(8)	N7	2.81
N10	C(9)	O2P**	2.91
N14	G(10)	N7**	3.16
N14		O6**	2.90
N14	18	W10	2.94
N14	18	W11	2.68

[a] The residue numbers and symmetry operators are in relation to the spermine molecule, surrounded by three symmetry-equivalent DNA duplexes. The symmetry operator for atoms with an asterisk is $(x + 1, y, z)$, and for those with a double asterisk, it is $(x + 0.5, -y + 0.5, -z + 1)$.

hydrogen bonds, and another O6 oxygen from the adjacent residue G(2) is situated 3.18 Å from the spermine nitrogen. The character of the latter interaction is mainly electrostatic, since carbon C13 and amino nitrogen N14 of spermine and the keto oxygen of guanine are arranged almost linearly. The other terminal amino nitrogen N1 of the interhelix spermine forms three hydrogen bonds as well. Two of them are to phosphate oxygens from backbones of two adjacent duplexes, and a third one is to a water molecule (Table 3). Both imino nitrogens are engaged in two hydrogen bonds. Whereas those of nitrogen N5 are to a phosphate oxygen and a water molecule, N10 is hydrogen bonded to a phosphate oxygen and a base nitrogen N7 from two adjacent residues. The interhelix

Table 4: Hydrogen-Bonding Interactions of the Intrahelix Spermine Molecule[a]

spermine	DNA/water		
atom (residue 14)	residue	atom	distance (Å)
N1	G(2)	O2P*	3.46
N1	18	W06	3.58
N1	20	W12	2.52
N5	C(1)	O2*	3.10
N5	C(7)	O2	2.82
N10	C(5)	O2	2.92
N10	C(9)	O2	3.07
N14	G(10)	O1P	2.64
N14	15	W02	3.08
N14	18	W08	2.86

[a] The residue numbers and the symmetry operator are in relation to the spermine molecule, interacting with two stacked DNA duplexes. The symmetry operator for atoms with an asterisk is $(-x + 1.5, -y + 1, z - 0.5)$.

spermine molecule is thus engaged in the maximum number of possible hydrogen bonds expected for a polyamine with four positively charged nitrogen atoms.

Intrahelix Spermine–DNA Interactions. The LT structure of the pure-spermine form of Z-DNA reported here differs from the previous RT structure by clear evidence of a second spermine molecule from Fourier electron density maps. This intrahelix spermine molecule is located within the continuous minor groove formed by two stacked Z-DNA duplexes and forms numerous contacts to the DNA and surrounding water molecules. Hydrogen-bonding distances between the intrahelix spermine molecule and DNA and water molecules are listed in Table 4. Views perpendicular and along the helical axis of DNA of the spermine binding in the minor groove are depicted in Figures 4 and 5, respectively, and a schematic diagram of the binding mode is shown in Figure 6A.

The central portion of the intrahelix spermine molecule assumes an almost extended conformation and is located close to the floor of the minor groove. The two imino nitrogens N5 and N10 each form two hydrogen bonds to O2 oxygens of adjacent cytosines from opposite strands. Both O2 oxygens contacted by spermine nitrogen N10 are located within the same helix, whereas the ones contacted by nitrogen N5 belong to stacked base pairs from two different duplexes. In both cases, one of the hydrogen bonds to the nitrogen atoms is slightly shorter and the other is slightly longer than 3 Å. Although all the hydrogen bond lengths fall into the optimal range expected for such interactions (Table 4), their directionality is not optimal due to the roughly parallel orientation of the long dimension of the intrahelix spermine molecule and an imaginary line connecting O2 oxygens of stacked cytosines in the Z-DNA minor groove.

The extended conformation of the central butyl chain of the intrahelix spermine molecule is interrupted by sharp bends at either end of the spermine molecule, resulting in an overall conformation which resembles a twisted U (Figures 1B and 5). Thus, the terminal nitrogen atoms of the intrahelix spermine molecule do not interact with the floor of the groove but rather contact phosphate groups from inside the minor groove (Figure 5). Nitrogen N1 forms a hydrogen bond to a phosphate oxygen of residue G(2), and nitrogen N14 forms a hydrogen bond to a phosphate oxygen of residue G(10). Consequently, the intrahelix spermine molecule spans two adjacent stacked duplexes. As shown in Figures 4 and 6A, one terminus of the spermine molecule including amino nitrogen N1 and the three adjacent methylene groups are

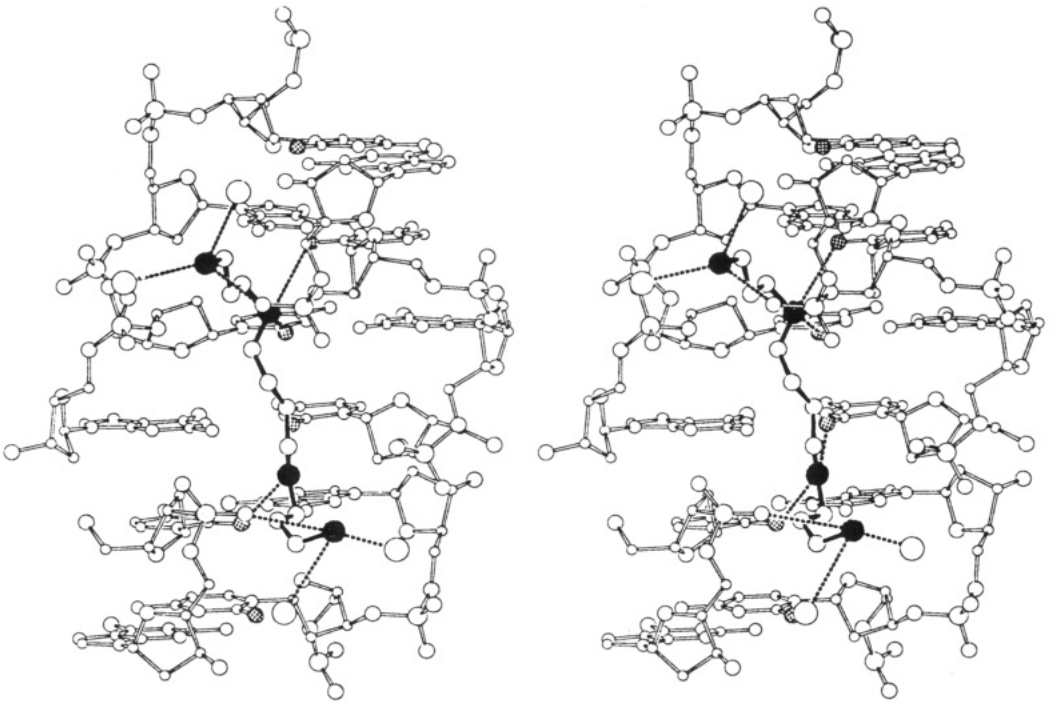

FIGURE 4: ORTEP stereodrawing of a view into the minor groove with the bound intrahelix spermine molecule and its first hydration sphere. The intrahelix spermine molecule binds to two stacked, symmetry-equivalent duplexes. The top four base pairs belong to one duplex and the bottom two to the second one. The missing phosphate groups between duplexes appear as the gaps in the backbones. N1 of spermine is located at the bottom. The DNA is drawn with hollow bonds, the spermine molecule with solid bonds, and hydrogen bonds are dashed. Atom types of the DNA are coded according to size with P > O > N > C. O2 oxygens of cytosines are stippled in gray, and amino and imino nitrogens of spermine are stippled in black. The largest circles are water molecules.

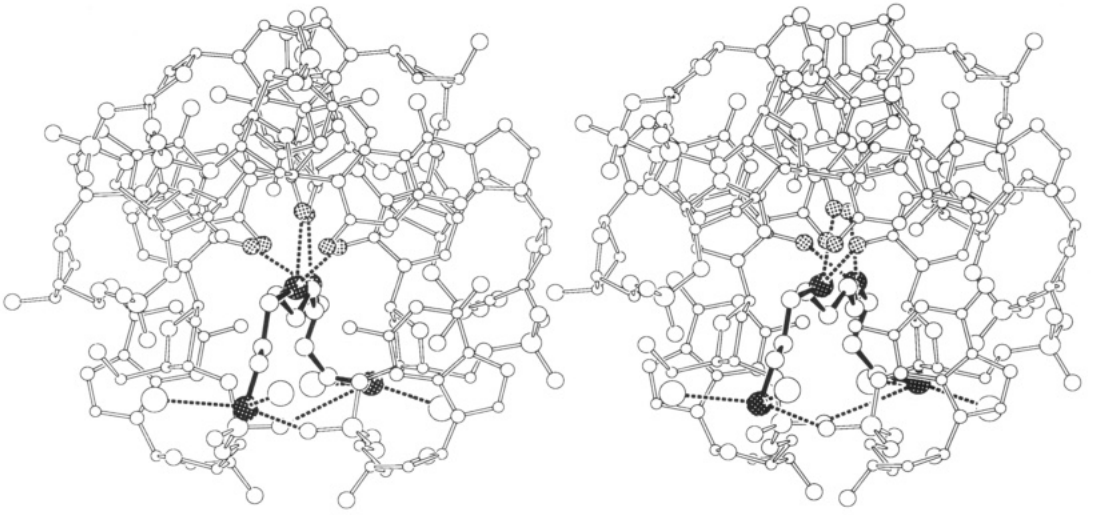

FIGURE 5: ORTEP stereodrawing of a view along the helical axis with the bound intrahelix spermine molecule and its first hydration sphere. Atom types and bonds are coded according to the convention described in the legend to Figure 4.

located within the minor groove of one duplex, while the rest of the molecule extends up to about half the length of the second duplex. Each of the terminal amino nitrogens of the intrahelix spermine forms two additional hydrogen bonds to water molecules. Like the interhelix spermine molecule, this spermine thus forms a total of 10 hydrogen bonds. Whereas the hydrogen-bonding distances indicate stable interactions between the DNA and the central portion of the spermine as well as one terminus, both lying in the minor groove of one duplex, the hydrogen bonds between N1 and the phosphate oxygen and one water molecule within the minor groove of the stacked duplex are rather long (3.46 and 3.58 Å, respectively, Table 4).

Minor Groove Hydration. In the crystal structures of the magnesium and mixed spermine/magnesium forms of $[d(CGCGCG)]_2$, a string of water molecules systematically bridges adjacent cytosine O2 oxygens from opposite strands in the minor groove. The water bridge is also present at the gap between stacked hexamer duplexes and is only missing between oxygens O2 of residues C(5) and C(7) in the mixed spermine/magnesium form. Thus a total of six water molecules are located at the floor of the minor groove. As visible in the projection of the duplex along the helical axis shown in Figure 5, the cytosine O2 oxygens form a more or less linear arrangement in the center of the left-handed duplex with distances between adjacent O2 oxygens ranging from 3.5 to 4.5 Å. The binding of the intrahelix spermine molecule in the minor groove disrupts this spine of hydration. Two of the six water molecules are replaced by the central imino nitrogens of spermine and two additional water molecules are

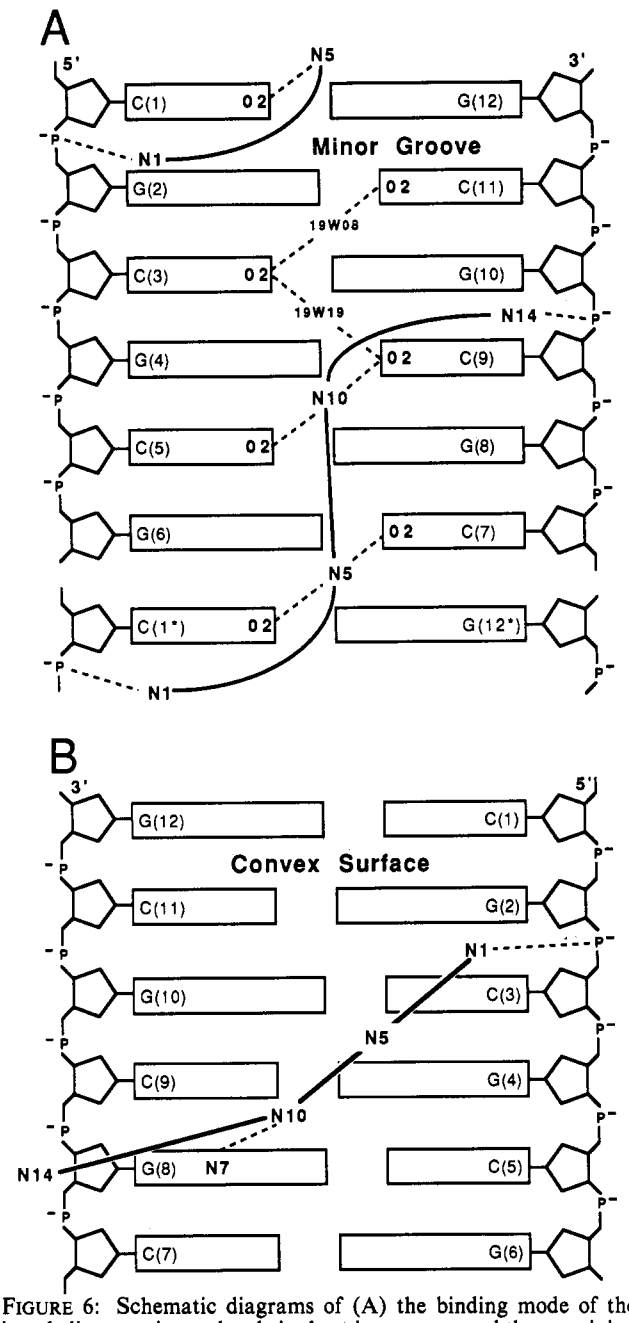

FIGURE 6: Schematic diagrams of (A) the binding mode of the intrahelix spermine molecule in the minor groove and the remaining spine of hydration, and (B) the binding mode of the interhelix spermine molecule on the convex surface. In panel A, one complete and one partial duplex, and one complete and one partial spermine molecule, are shown. In panel B one complete duplex is shown, but this spermine molecule forms hydrogen bonds to two additional duplexes (not shown). Hydrogen bonds between spermine amino and imino nitrogen atoms and the DNA or water molecules are dashed.

displaced. Only two of the six water molecules normally forming the hydration spine are observed in the LT pure-spermine form (Figures 4 and 6A). Specifically, imino nitrogen N10 replaces the water molecule that bridged oxygens O2 of residues C(5) and C(9), and imino nitrogen N5 replaces the water molecule that bridged oxygens O2 of residues C(7) and C(1)*, linking two stacked, symmetry-related duplexes. Two additional water molecules of the hydration spine are displaced by methylene groups of the intrahelix spermine molecule. These water molecules normally bridge the O2 oxygens of residues C(5) and C(7), and C(1) and C(11), respectively. In the LT structure of the pure-spermine form, water molecule W08(19) is hydrogen bonded to O2 of residue C(3) (2.85 Å) and O2 of residue C(11) (2.81 Å). The other remaining water molecule of the former spine of hydration is W19(19), which bridges O2 of residue C(3) (3.11 Å) to O2 of residue C(9) (3.28 Å).

Across the minor groove, one or two water molecules link N2 nitrogens of guanine residues to the phosphate groups, lying on the 5′ and the 3′ side of the guanosines (the 3′-phosphate group is formally assigned to the next residue). This pattern is also observed in the LT structure of the pure-spermine form, where three of the six N2 nitrogens of guanines are linked to the 3′-phosphate groups by two water molecules. Because the phosphate groups between stacked duplexes are missing, the water bridges from the N2 nitrogens of residues G(6) and G(12) end at phosphate groups of symmetry-related, parallel duplexes instead. In two cases [residues G(2) and G(10)], a single water molecule bridges N2 nitrogens and 3′-phosphate groups, and, in the case of residue G(8), the water bridge is missing due to adoption of a partial Z_{II} conformation of phosphate P9 (this results in a significant elongation of the distance between N2 and the phosphate oxygen). The binding of the intrahelix spermine molecule in the minor groove therefore does not appear to distort the formation of water bridges between guanine N2 nitrogens and phosphate groups located on the 3′ side.

Whereas the above water bridges to 3′-phosphate groups are located more or less within the plane of the base pair, an imaginary line between N2 nitrogens of guanosine residues and their 5′-phosphate groups would run along the minor groove, parallel to the direction of the bound spermine molecule. As mentioned before, both the RT and LT pure-spermine form Z-DNA duplexes are compressed along the helical axis, with slightly reduced distances between stacked base pairs. This compression leads to shorter distances between N2 nitrogens and 5′-phosphate oxygens in this form compared to the magnesium and mixed spermine/magnesium forms. The average N2–O(P) distance in the pure-spermine form duplex is 0.25 Å shorter compared to the mixed spermine/magnesium form, and it is 0.1 Å shorter compared to the magnesium form. While four of the six water bridges of this type in the magnesium-containing forms comprise two water molecules, four N2 nitrogens in the LT structure of the pure-spermine form are bridged to 5′-phosphate oxygens by a single water molecule. In the case of residue G(2), nitrogen N2 and the phosphate oxygen are bridged by a water molecule and spermine amino nitrogen N1, and, in the case of residue G(10), they are bridged by a water molecule and amino nitrogen N14. Thus, binding of the intrahelix spermine molecule does not fundamentally alter the stabilizing water structure in the minor groove. Except for a portion of the longitudinal spine of hydration close to the floor of the groove, the water network is intact with all four positively charged spermine nitrogens replacing specific water molecules and mediating hydrogen bonds in their place.

Sodium Ions. In addition to the two spermine molecules, two sodium ions were found in the lattice of the LT pure-spermine form. The 10 negative charges of the phosphate groups of the hexamer duplex are therefore fully neutralized in the structure described here. Sodium ions were assigned after an analysis of the number of nearest neighbors around water molecules and the distances between them. Near the end of the refinement, two water molecules were observed to be surrounded (within 3.0 Å) by six neighbors. These two water molecules were reassigned as sodium ions and refined without applying any distance or angle restraints. Both sodium ions display pseudo-octahedral coordination geometry. Dis-

Table 5: Coordination of Sodium Ion 1

sodium ion 1 (residue 15)	DNA/water residue	atom	distance (Å)
Na^+	C(5)	O1P	2.66
	15	W01	2.92
	15	W02	2.76
	15	W03	3.02
	15	W04	2.98
	15	W05	2.90

Table 6: Coordination of Sodium Ion 2

sodium ion 2 (residue 16)	DNA/water residue	atom	distance (Å)
Na^+	C(5)	O1P	2.98
	C(5)	O2P	2.80
	15	W02	2.79
	16	W01	2.81
	16	W02	2.61
	16	W03	2.75

tances between sodium ion and water molecules as well as DNA atoms are listed in Table 5 for sodium ion 1 and in Table 6 for sodium ion 2. Figure 7 depicts portions of two stacked hexamer duplexes, the intrahelix spermine molecule, and the two coordinated sodium ions.

Sodium ion 1 is surrounded by five water molecules and phosphate oxygen O1P of residue C(5). Sodium ion 2 is surrounded by four water molecules and both phosphate oxygens from the above phosphate group of residue C(5), as well as by O3′ of residue G(4) (distance 2.84 Å). Two bridges link the sodium ions. Water molecule W02(15) and O1P of residue C(5) both interact simultaneously with both sodium ions. Three water molecules that bind to sodium ions form hydrogen bonds to amino and imino nitrogens of spermine molecules. Water molecule W02(15) is located 3.08 Å from N14 of the intrahelix spermine molecule, water molecule W03-(15) is located 2.82 Å from N1 of the interhelix spermine molecule, and water molecule W01(15) is located 2.86 Å from N5 of the interhelix spermine molecule. Thus, the sodium ions and the three positively charged amino and imino nitrogens of spermine molecules form a cluster of positive charges. This cluster of positive charges is surrounded by 10 negatively charged phosphate groups, each falling within a sphere of radius 10 Å. The center of the sphere is approximately midway between the two sodium ions. A total of three symmetry-related duplexes contribute phosphate groups to this sphere. The sodium ions and the spermine ammonium nitrogens are part of a dense hydrogen-bonded network. Each of the water molecules in the coordination shell of the two sodium ions participates in four hydrogen bonds. In each case at least one of these hydrogen bonds is to a phosphate oxygen or to a base atom of the DNA (N7 of guanine or N4 of cytosine).

Molecular Motion. Cooling the crystal to −110 °C results in significantly lower isotropic temperature factors (*B* factors) for individual atoms compared to the RT structure. Individual *B* factors of DNA atoms at LT are about 25% lower than the *B* factors of corresponding atoms in the RT structure. In the LT structure, *B* factors of DNA base atoms lie between 4.5 and 8 Å^2, those of deoxyriboses lie between 6 and 9 Å^2, and *B* factors of phosphate groups (atoms P, O1P, O2P, O5′, and O3′) are highest, ranging from 6 to 14 Å^2. As in the RT structure, phosphate P9 displays disorder, and its thermal motion in the LT structure is comparable to that in the RT one.

The thermal motions of the two termini of the interhelix spermine molecule differ considerably in the RT as well as in the LT structure. The terminal amino nitrogen N1 forms hydrogen bonds to two phosphate oxygens of backbones from neighboring duplexes, and terminal amino nitrogen N14 forms hydrogen bonds to atoms N7 and O6 of a guanine base. The *B* factor of N14 is almost twice as high as the one of N1. One might expect the temperature factors of atoms in the portion of spermine contacting the backbone to be slightly higher than those of atoms in the one contacting base atoms. However, the average *B* factor of the phosphate groups contacted by nitrogen N1 is only slightly higher than the one of the base atoms of residue G(10), contacted by N14. Moreover, the *B* factors of bases, deoxyriboses, and phosphates differ only slightly as a function of their location in the pure-spermine form duplex. Also, a comparison of the hydrogen-bond distances in the three instances indicates that hydrogen bonds between positively charged nitrogens and phosphate oxygens are stronger than those between the nitrogens and DNA base atoms. The lower *B* factors of the atoms in the spermine terminus contacting two phosphates groups compared to the other terminus may therefore not be unexpected. In addition, different restrictions imposed on the two termini by the deviating chemical environments in the lattice may influence thermal motion as well.

The intrahelix spermine molecule displays higher thermal motion than the interhelix spermine molecule. The average *B* factor of interhelix spermine atoms is 10 Å^2 whereas the average *B* factor of intrahelix spermine atoms is 34 Å^2. This difference may simply indicate higher thermal motion of the spermine molecule in the minor groove compared to the spermine arranged between duplexes but may also be caused by partial occupancy of the intrahelix spermine. The sum electron density around the interhelix spermine is clearly better resolved than the density around the intrahelix spermine (Figure 1B,C). Also, it should be noted that there was no evidence for a bound spermine molecule in the minor groove from electron density maps calculated with the RT data. During the refinement of the LT structure, various arrangements of the spermine molecule within the minor groove were modeled and refined, since the electron density maps in that region did not permit a completely unambiguous positioning of the second spermine molecule. However, the final orientation and conformation of the intrahelix spermine was clearly superior to the tested alternatives, in terms of both the *R* factor and the resulting electron density maps. Because of the above observations, the relatively high *B* factors of the intrahelix spermine atoms can most likely be attributed to partial occupancy of this spermine.

The position of a water molecule is restrained to a greater extent by two or three hydrogen bonds to the DNA than by a single hydrogen bond. In the LT structure of the pure-spermine form, water molecules which form only a single hydrogen bond to the DNA show higher *B* factors than water molecules forming two or three hydrogen bonds to the DNA. One water molecule forms three hydrogen bonds to the DNA, and its *B* factor is 13 Å^2. A total of 21 water molecules, with an average *B* factor of 24 Å^2, each form two hydrogen bonds to the DNA , and 32 water molecules, with an average *B* factor of 28 Å^2, each form a single hydrogen bond to the DNA.

Crystal Lattice. For the RT structure of the pure-spermine form, unit cell constants *a* and *c* differed considerably from those of all other Z-DNA hexamer crystals (Egli et al., 1991). The unit cell volume of that structure was reduced by about 3% compared to the one of the mixed spermine/magnesium

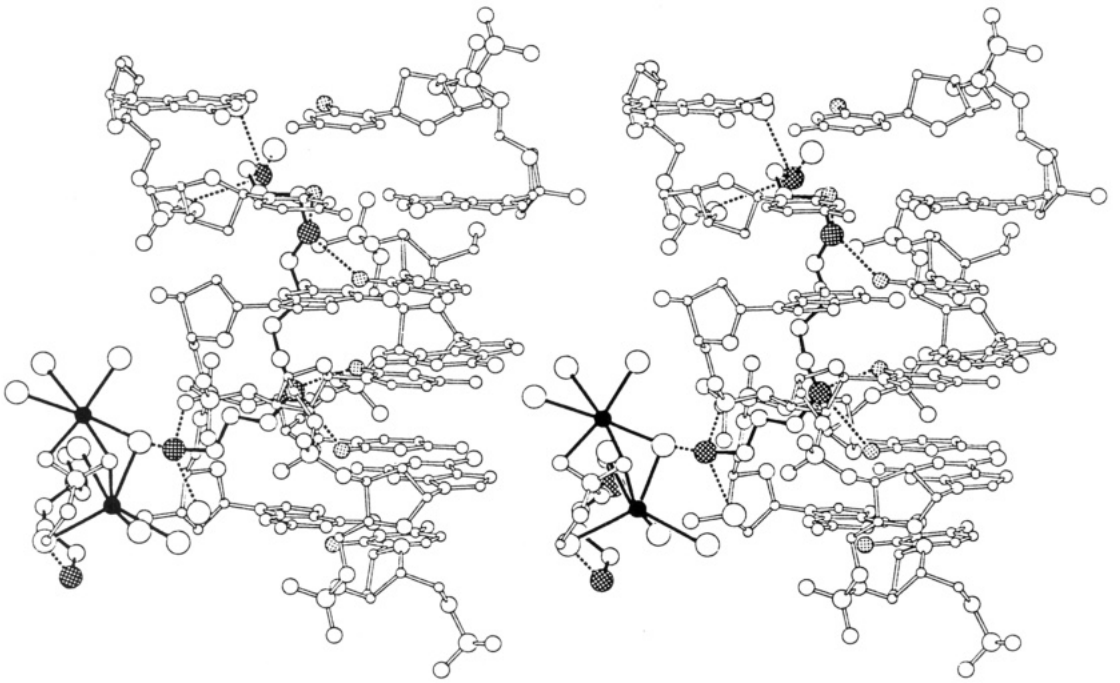

FIGURE 7: ORTEP stereodrawing of the view in Figure 4, rotated by about 90° around the vertical, showing the bound intrahelix spermine molecule and the two hydrated sodium ions. Atom types and bonds are coded according to the convention described in the legend to Figure 4. Sodium ions are black and connected to the coordinating water molecules and DNA backbone atoms via solid lines. The chain of atoms drawn with solid bonds at the bottom left belongs to the interhelix spermine molecule, and a portion of the backbone of a symmetry-related duplex is represented with open bonds.

form. Compared to the RT structure, the LT structure *a* cell constant is 0.14 Å (0.8%) shorter, the LT *b* cell constant is 0.08 Å (0.3%) shorter, and the LT *c* cell constant is 0.70 Å (1.6%) shorter. Thus, cooling results in additional decrease of the unit cell volume by approximately 3%. In the RT as well as in the LT structure, the decrease results primarily from compression along the helical axis (the crystallographic *c* axis). Thus the helical axis is compressed by nearly 5% in the LT pure-spermine form compared to the mixed spermine/magnesium form (RT measurement).

In the RT structure, a total of 47 ordered water molecules were found, and the water content of the crystals was 18% (w/w). The calculated density of the crystals based on this structure was 1.26 g/cm^3 and thus considerably smaller than the calculated densities of the mixed spermine/magnesium and magnesium form crystals (1.41 and 1.37 g/cm^3, respectively). In the LT structure, a total of 62 ordered water molecules were detected, which corresponds to a water content of the crystals of 21% (w/w). The calculated density of the pure-spermine form crystals based on the LT structure is 1.43 g/cm^3, and thus slightly higher than the ones of the magnesium ion containing crystals. This number includes the intrahelix spermine molecule and two sodium ions whose positions could be determined using the LT data set, which yields sharper and better-defined electron density maps. Thus, the 10 negative charges of the phosphate groups of the hexamer duplex are fully neutralized in the LT structure of the pure-spermine form.

Viewing the crystal lattice along the direction of the helical axis reveals that each duplex is nearly surrounded by positive ions (Figure 8). In addition, each duplex contains a positive charge of four within its minor groove, contributed by portions of two symmetry-related intrahelix spermine molecules. The DNA duplexes stack with 3′–5′, 5′–3′ overlap to form infinite helices in the lattice. These infinite helices, which form a pseudohexagonal arrangement are well hydrated, with solvent channels separating them in the lattice. Two distinct types

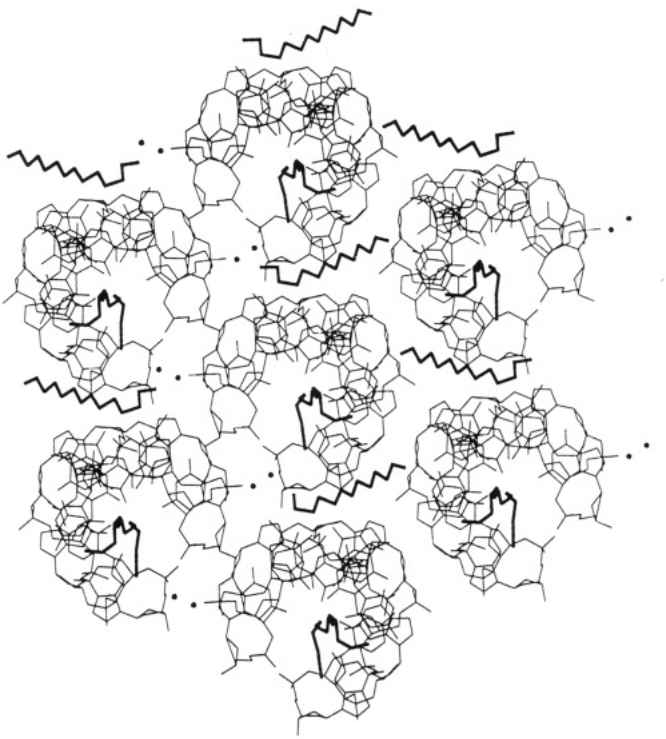

FIGURE 8: Packing arrangement in the crystal lattice of the LT pure-spermine form viewed along the crystallographic *z*-axis. The drawing shows an *xy* layer (*x*-axis vertical; *y*-axis horizontal) of approximately 20 Å thickness centered around $z = 3/4$. Each duplex (plus two bound spermine molecules and two sodium ions) is surrounded by six other duplexes (plus bound ions) within the layer. The DNA is drawn with thin lines, the spermine molecules are drawn with thick lines, and the dots are sodium ions. Water molecules have been omitted.

of channels are generated. In the layer of duplexes shown in Figure 8, the walls of one type are formed by convex surfaces of three adjacent duplexes. These channels contain the

interhelix spermine molecules. The walls of the other channel type are formed by the convex surfaces of two adjacent duplexes and the phosphate backbones rimming the minor groove of a third one. These channels contain the hydrated sodium ions.

DISCUSSION

Data from the pure-spermine form of Z-DNA collected at RT revealed only a single spermine molecule in the Fourier electron density maps (Egli et al., 1991). This interhelix spermine molecule contacted three neighboring helices in the crystal lattice. The spermine conformation changes slightly in the LT crystal structure. The largest positional shift occurs at one terminus, placing amino nitrogen N14 closer to oxygen O6 of residue G(10) and away from nitrogen N7 of the same residue. In the RT structure, the spermine amino nitrogen was located almost equidistant from these two atoms. Data collected at LT also reveal two additional water molecules in the vicinity of this spermine terminus, and the protonated amino and imino nitrogen atoms of the interhelix spermine molecule are engaged in a total of 10 hydrogen bonds. In the case of two duplexes, the spermine contacts are mainly to functional groups of bases on the convex surface and to phosphate groups bordering it. In addition, the spermine molecule runs along the minor groove of a third duplex. All the contacts to phosphate oxygens occur from the outsides of duplexes, and none of the positively charged nitrogen atoms of the interhelix spermine protrude into the minor groove. This spermine molecule neutralizes repulsive phosphate interactions between helices and thus mediates close contacts between them in the crystal lattice.

A second spermine molecule, the intrahelix spermine molecule, observable at LT but not at RT binds within the minor groove and interacts with two stacked hexamer duplexes in the lattice. At LT the molecular motion within a crystal is significantly reduced compared to RT, and Fourier electron density maps calculated with LT data correspondingly may reveal finer details. When a macromolecule crystal is cooled, the effects on the quality of the X-ray data appear to depend on the initial crystal quality and other parameters such as the degree of hydration. In the first low-temperature crystallographic study, crystals of the B-DNA dodecamer d(CGCGAATTCGCG) were cooled to 16 K very slowly (Drew et al., 1982). Although the resolution of that structure was relatively low (ca. 2.5 Å), the number of water molecules observable in the Fourier electron density maps increased dramatically upon cooling. In a recent application of the flash freezing method with crystals of the A-DNA octamer d(GGGCGCCC), a larger proportion of unobserved reflections at LT (115 K) compared to RT was reported (Eisenstein et al., 1988). Also, the reflection profiles (ω scan) were about twice as wide, and the final R factor was 5% higher than the one at RT. In contrast, in the case of crystals of the pure-spermine form of Z-DNA, cooling increases the number of observed reflections by 17% over the RT data (Table 1) and has little effect on the width of the reflection profiles. Cooling increases the number of ordered solvent molecules by over 30% compared to the RT structure. The R factor of the LT structure is slightly lower than that of the RT structure.

The observed differences between the RT and LT structures in the present case demonstrate that the interpretation of the interactions of biopolymers with the surrounding solvent in crystals may vary considerably as a function not only of resolution but also of temperature. Z-DNA forms more highly ordered and better diffracting crystals than all other oligomers of DNA and nearly all proteins. The X-ray data obtained at RT from the pure-spermine form crystals were of very high quality (resolution = 1.0 Å, overdeterminacy ratio = 6.8). Even with such data, a bound spermine molecule in the minor groove gave the appearance of a spine of hydration in the Fourier electron density maps at RT. The presence of the spermine molecule, as determined by the LT data, was not indicated in the RT maps. Their retrospective analysis indicates that the shape of the $2F_o - F_c$ sum electron density surrounding those water molecules which were incorrectly assigned to the spine of hydration is not ideally spherical but still within the range used for other water molecule assignments in the maps. It may be reasonable to reconsider the minor groove water molecule assignments in other DNA crystal structures. Unfortunately, B-DNA crystals diffract X-rays at best to 1.3-Å resolution, and more generally to between 2 and 3 Å. It is conceivable that spermine molecules were improperly described as water molecules in these resolution ranges.

Conformational Adjustments of the DNA. The binding of the intrahelix spermine molecule within the minor groove induces a conformational adjustment of the DNA, increasing the depth of the minor groove by about 1 Å, decreasing the width of the groove by 1 Å, and compressing the helix by roughly the same amount. The two central imino nitrogens of the intrahelix spermine molecule form four hydrogen bonds to O2 oxygens of four successive cytosine bases from opposite strands in the minor groove. These interactions cause the bases to shift away from the minor groove, indicated by significantly higher values for x displacement for base pairs in the LT pure-spermine form duplex compared to the magnesium and mixed spermine/magnesium form duplexes. This shift of bases away from the minor groove toward the convex surface alters the position of the helical axis. When spermine is absent from the minor groove (as in the magnesium and mixed spermine/magnesium forms), the helical axis passes through O2 positions of cytidines. However, in the pure-spermine form the helical axis is located within the minor groove. The decrease in the width of the groove is a consequence of the reduced cross-groove electrostatic repulsion between phosphate groups upon insertion of four positively charged nitrogen atoms between the phosphates. The contraction of the duplex by about 5% along the helical axis is very likely a direct consequence of the binding of the spermine molecule within the minor groove. The spermine molecule covers four consecutive base pairs in the minor groove. The constraints presented by the propyl and butyl groups linking the positively charged nitrogens require conformational adjustments of both the spermine and the DNA in order to allow for optimal hydrogen-bonding interactions between the two. The differences between the extentions of the spermine molecule arranged along the minor groove and the extensions of stacked base pairs in the DNA seem to be the cause for the shortening of the duplex in the pure-spemine form crystal. To our knowledge this is the first X-ray crystallographic observation of a spermine-induced conformational change of DNA.

The Intrahelix Spermine Binding Mode. The environments of the central imino and terminal amino nitrogens of spermine upon binding to the minor groove of the left-handed double helix are quite different. Whereas both imino nitrogens are arranged close to the floor of the groove and between O2 oxygens of adjacent cytosine bases, the amino nitrogens are located at the periphery of the minor groove and close to phosphate oxygens. Although the imino nitrogens are not hydrogen bonded to phosphate oxygens, they are both in the

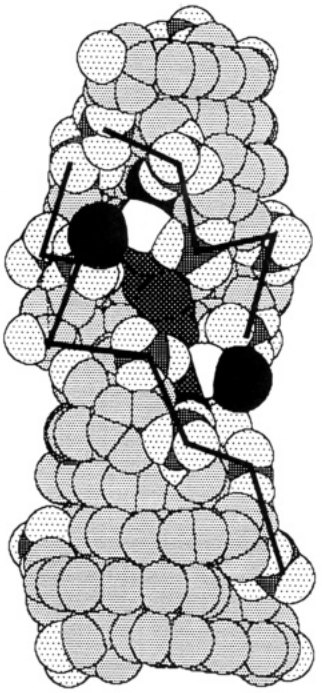

FIGURE 9: Van der Waals representation of the intrahelix spermine molecule bound to two stacked Z-DNA hexamer duplexes, viewing into the minor groove. DNA carbon, nitrogen, and oxygen atoms are stippled in gray, phosphorus atoms are stippled in black, and oxygen atoms of phosphate groups are stippled lightest. Spermine carbon atoms are stippled darkest, and terminal amino nitrogen atoms are white (both imino nitrogen atoms are hidden by the spermine methylene chains). Water molecules hydrogen bonded to spermine amino groups are black, and the phosphorus atoms in both backbones are traced with solid lines.

vicinity of two phosphate groups. Imino nitrogen N5 is located 5.13 Å from phosphorus P8 and 5.44 Å from phosphorus P2* (the asterisk designates the symmetry-related, stacked duplex; N5 is bridging O2 oxygens from two duplexes, see Figure 4 and Table 4). Imino nitrogen N10 is located 5.25 Å from phosphorus P6 and 5.23 Å from phosphorus P10. These distances are just slightly longer than those between the terminal amino nitrogens and the phosphorus atoms surrounding them (see below). Thus, the location of the imino nitrogens, with the more obvious function of linking O2 oxygens from adjacent cytosine bases, in addition furnishes a significant electrostatic contribution. Each of the two amino nitrogens lies in the vicinity of three phosphate groups, whereby one of the phosphate groups is contacted directly via a hydrogen bond. This is visible from Figure 9 which depicts a space-filling model of the complex between the stacked Z-DNA hexamers and the intrahelix spermine molecule. In the case of amino nitrogen N1, these three phosphorus atoms are P2* (4.73 Å), P3* (6.30 Å), and P8 (4.60 Å; N–P distances in parentheses). The hydrogen bond is to phosphate oxygen O2P* of residue G(2) (Table 4), and the two water molecules hydrogen bonded to N1 link this nitrogen to the two other phosphate groups. Water molecule W06(18) bridges N1 and phosphate P3* with hydrogen-bonding distances to nitrogen and phosphate oxygen of 3.58 and 2.89 Å, respectively. Water molecule W12(20) bridges N1 and phosphate P8 with a hydrogen-bonding distance to the nitrogen of 2.52 Å and a rather long contact of 3.99 Å to the phosphate oxygen. In the case of amino nitrogen N14, the three neighboring phosphorus atoms are P10 (3.92 Å), P6 (5.83 Å), and P11 (5.54 Å; N–P distances in parentheses). The hydrogen bond is to phosphate oxygen O1P of residue G(10) (Table 4), and the two water molecules hydrogen bonded to N14 link this nitrogen to the two other phosphate groups. Water molecule W02(15) bridges N14 and phosphate P6 with hydrogen-bonding distances to nitrogen and phosphate oxygen of 3.08 and 3.32 Å, respectively. Water molecule W08(18) bridges N14 and phosphate P11 with hydrogen-bonding distances to nitrogen and phosphate oxygen of 2.86 and 2.79 Å, respectively.

The contacts of the intrahelix spermine molecule, as well as those of the interhelix spermine molecule, to the DNA occur exclusively via hydrogen bonds. The interactions do not appear to involve any large hydrophobic component. This lack of interactions of spermine methylenes with hydrophobic regions of Z-DNA contrasts sharply with the interactions of spermine molecules bound to A-DNA (Jain et al., 1989) or to B-DNA–anthracycline complexes (Williams et al., 1990). In those complexes many methylene groups of spermine molecules are in close contact with methyl groups of thymidine residues.

The analysis of the intrahelix spermine binding mode indicates that there are in fact several possible alternative arrangements of the spermine within the minor groove, which would reduce repulsions between phosphate groups from opposite strands in a comparable way. Such alternatives could involve both local conformational changes of the spermine molecule as well as a translation of the entire molecule along the groove, or a combination of the two. In Figure 9, the alternating widening and contracting of the minor groove has been emphasized by connecting the phosphorus atoms along each strand with solid lines. In the Z-DNA duplex, the phosphate groups of guanosine residues are closely spaced across the groove. The two amino nitrogens are located at two neighboring minor groove sites of maximal contraction (Figure 9), thus neutralizing cross-groove electrostatic repulsions most effectively and allowing significant stabilization of the duplex. Judging from the distances between the terminal amino nitrogens and two of the three phosphate groups surrounding each of them (the ones which belong to guanosine residues), the direct hydrogen bonds from the nitrogens could be established to either of them in both cases. Thus, although N1 is hydrogen bonded to phosphate P2*, the aminopropyl group at this end of the spermine molecule could swing over and its nitrogen could form a direct hydrogen bond to phosphate P8 from the opposite strand of the stacked duplex. Similarly, the other terminus with nitrogen N14 could swing over to form a direct hydrogen to phosphate P6, instead of the observed one between N14 and phosphate P10. Alternatively, the spermine molecule could shift along the minor groove by a two base pair step and still maintain favorable electrostatic interactions with the DNA via its amino and imino nitrogens. For example, amino nitrogen N1 would then be placed at the former location of amino nitrogen N14, and the latter would be placed at an adjacent site of maximal contraction of the backbones rimming the minor groove (see Figure 9). The two central imino nitrogens would be shifted to two O2 oxygens from neighboring cytosine residues. Such a shift would place the spermine molecule within the minor groove of a single duplex, rather than within the continuous groove generated by two adjacent duplexes, as observed in the pure-spermine form LT structure reported herein.

The existence of several possible arrangements of the spermine molecule in the minor groove, resulting in either similar or apparently identical stabilities of the spermine–DNA complex, is consistent with the relatively high mobility of the intrahelix spermine molecule in the present structure. There is no obvious reason why the spermine molecule is predominantly found between two duplexes, rather than

interacting with a single duplex. The superposition of the top [base pairs C(1)·G(12), G(2)·C(11), and G(3)·C(10)] and bottom halfs [base pairs G(4)·C(9), C(5)·G(8), and G(6)·C-(7)] of the duplex results in an RMS deviation of 0.78 Å. This does not suggest a dramatic difference between the conformations of the two duplex portions, interacting with different termini of the intrahelix spermine molecule. Moreover, the largest deviation is contributed by the superposition of two backbone phosphate groups, of which one adopts a partial Z_{II} conformation and the other one is in the normal Z_I conformation. A reason for the preference for an arrrangement between stacked duplexes may be the higher conformational flexibilty of the backbone at the end of a duplex due to the absence of geometrically constraining phosphate groups linking hexamer duplexes at that site.

The arrangement of the intrahelix spermine molecule and its interactions with minor groove functional groups reveal the advantages of a butyl group linking the central imino nitrogens compared to a propyl group. Although the protons of two nitrogens at the ends of a propyl group adopting an *all-trans* conformation point to the same side, model building suggests that the propyl group is too short for an optimal positioning of the imino nitrogens with respect to pairs of two O2 oxygens of four adjacent cytosine bases from opposite strands but too long to simply bridge two cytosine O2 oxygens from neighboring base pairs. In addition to being too short, each nitrogen at the end of a propyl group could only form one stable hydrogen bond each to an O2 oxygen. Conversely, a butyl group is long enough to allow the imino nitrogens to interact with a total of four O2 oxygens. Although the protons of two nitrogens at the ends of a butyl group adopting an *all-trans* conformation point to opposite sides, rotation around two carbon–carbon bonds in the central portion into an *ac* torsion angle range allows the spermine molecule to adapt to the helical twist of the DNA and place both imino nitrogens in an optimal location for the formation of two hydrogen bonds to O2 oxygens per imino nitrogen. Rather than contacting two additional O2 oxygens from cytidines at the floor of the groove, the two propyl chains at both ends of the spermine molecule fold back toward the phosphate backbones. The resulting interactions between amino nitrogens and phosphate groups (some of them water-mediated) supposedly lead to higher stability of the complex compared to that of an arrangement with just two additional hydrogen bonds to cytidine oxygens.

Implications for the B-DNA to Z-DNA Transition. In previous crystal structures of complexes between various mono-, di-, and polyvalent cations and Z-DNA hexamer duplexes $[d(CGCGCG)]_2$, ion binding sites were restricted to the convex surface and the phosphate groups. In the mixed spermine/magnesium (Wang et al., 1979) and magnesium forms (Gessner et al., 1989), hydrated magnesium ions formed hydrogen bonds to guanine O6 and N7 functions on the convex surface. Similar interactions were also observed in the crystal structure of a Z-DNA hexamer stabilized by magnesium and hexaamminecobalt ions (Gessner et al., 1985). A characteristic of the complexes between Z-DNA and di- and trivalent metal cations is the clustering of such ions on the convex surface (Wang et al., 1984; Gessner et al., 1985). Although divalent metal cations have not been observed to bind within the minor groove thus far, they seem to preclude binding of spermine in that region. For example in the mixed spermine/magnesium form, two crystallographically distinct spermine molecules bind to the DNA (Wang et al., 1979). However, neither of these spermine molecules protrudes into the minor groove. Earlier crystal structures of complexes between spermine as well as other polyamines and Z-DNA have established a number of preferred binding sites of the ions along the left-handed duplex. These comprise the guanine O6 and N7 functions on the convex surface and the phosphate groups (Wang et al., 1979; Tomita et al., 1989; Egli et al., 1991) as well as water-mediated contacts by a terminal amino nitrogen to O2 oxygens in the minor groove (Ohishi et al., 1991). In general, these structures revealed a tendency of the spermine molecule to lie across or between two or three neighboring duplexes, rather than interacting with a single duplex.

Structural considerations suggest that spermine and magnesium would differ significantly in the manner in which they stabilize and facilitate close intermolecular approaches of nucleic acids. Spermine is long (over 14 Å from end to end) with functional groups that are both spatially dispersed and polymorphic in their mode of interaction (charge–charge, hydrogen bonding, hydrophobic). Thus spermine contains the potential to simultaneously interact with many nucleic acid molecules (a spermine molecule interacts with three in the present structure) by many different interaction modes. The dispersion of charge over the length of the molecule is consistent with the binding of the intrahelix spermine in the minor groove, where the electronegative potential is extended and shallow. The binding to a region of extended but relatively poorly defined electronegative potential may be another reason for the high temperature factors of the intrahelix spermine molecule. In contrast to spermine, the hydrated magnesium ion is compact, with localized charge and more rigid directionality of hydrogen-bonding groups. The mode of interaction is less polymorphic with no potential for hydrophobic contributions. Magnesium ions are likely to bind with the greatest stability in regions of deep and well-defined electronegative potential.

The midpoints of the B-DNA to Z-DNA conformational transition with poly(dG–m^{5}dC)·poly(dG–m^{5}dC) occur at different concentrations, depending on the nature of the ions used: 0.7 M NaCl, 0.6 mM $MgCl_2$ (in the presence of 50 mM NaCl), 5 μM $Co(NH_3)_6^{3+}$, and 2 μM spermine (Behe & Felsenfeld, 1981). In the case of the two latter ions, the transitions are complete at 7 and 4 μM concentrations, respectively. At the DNA concentrations used in these experiments, the end points correspond to 2 positive charges per phosphate group in the case of hexaamminecobalt and 0.3 positive charge in the case of spermine. The higher charge as well as the formation of more and specific hydrogen bonds, with simultaneous binding of the cobalt complex to DNA base atoms and a phosphate group, were found to be the cause of the great effectiveness of hexaamminecobalt in stabilizing Z-DNA (Gessner et al., 1985). Calculating the number of positive charges per phosphate group contributed by the intrahelix spermine molecule in the pure-spermine form LT structure, one obtains values of between 0.3 and 0.4 (depending on whether one includes 10 phosphates per duplex or rather assumes 12 to account for the infinite character of the duplex columns in the lattice). This is in good accordance with the above experimental value from titration studies with Z-DNA polymer in solution. Other results show that the transition from B to Z of poly(dG–m^{5}dC)·poly(dG–m^{5}dC) will occur with as little as one spermine molecule bound per 40–50 nucleotides (using 1 mM Na^+ concentrations and less) (Chen et al., 1984).

From the drastic differences between various ions in inducing the B–Z transition, it appears reasonable to assume that the

transition is governed by specific individual interactions between these ions and the DNA surface or by differential stabilization of the DNA surface hydration (Chen et al., 1984). This would make the B–Z transition a thermodynamically controlled process, whereby ions affect the equilibrium through their different binding energies to the B and Z forms. The intrahelix spermine binding mode in the present structure strongly supports this assumption. The binding mode within the minor groove suggests a more effective stabilization of the spermine Z-DNA complex compared to those between di- and trivalent hydrated metal cations and Z-DNA, as well as compared to those between various interhelix binding-type polyamines and Z-DNA, cited above. In addition, binding of the intrahelix spermine molecule in the minor groove contributes a favorable entropy component to Z-DNA formation by releasing water molecules from within the minor groove. The conclusion that spermine facilitates the B–Z transition by forming a stable complex with the Z-form rather than through a partial kinetic control, as proposed recently (Haworth et al., 1992), is also supported by the observation that the rates at which polyamines induce the transition is still very low (Basu et al., 1990).

The pure-spermine form LT crystal structure provides some qualitative rationalization for the differing efficiencies by which various polyamines induce the conformational transition. The tetraamine spermine and the pentaamine 4-4-4-4 (the numbers correspond to the length of the alkyl chains linking the nitrogens) induce the transition with particular efficiency (Basu et al., 1990). The same researchers found a decrease in efficiency both with tetraamines with an increased (3-8-3) and a decreased (e.g., 3-3-3 and 3-2-3) length of the central alkyl chain relative to spermine (3-4-3). Furthermore, the pentaamine 3-3-3-3 was found to be the only cation with more than two positive charges that could not induce a complete transition (Basu & Marton, 1987). In general, the experimental results suggest a crucial importance of at least one *n*-butyl group linking nitrogens within the polyamine (Basu & Marton, 1987; Thomas & Messner, 1988), whereby the position of the butyl group within the molecule seems to have little effect on the efficiency to induce the transition (Basu & Marton, 1987). The superiority of interactions between minor groove functions and positively charged nitrogens linked by a butyl group over those resulting from nitrogens linked by a propyl group have been pointed out in the previous section. Such conclusions drawn from a single structure, offering an explanation based simply on the observation of the detailed interactions between a particular polyamine and Z-DNA, are by no means sufficient, however, to understand further molecular determinants of polyamines affecting the B–Z transition. Among those are the molecular valency, charge deletion sites, steric bulk, and steric group location, to mention just a few (Vertino et al., 1987). A more detailed understanding of the role of polyamines in the promotion of the structural transition requires the crystallization of complexes between further polyamines and left-handed DNA fragments and their structure determination at sufficient resolutions to unravel the molecular interactions.

Spermine has never been observed crystallographically in complexes with native B-DNA at resolutions comparable to the structure described here. A spermine molecule was tentatively identified in a complex with a B-DNA dodecamer (Drew & Dickerson, 1981) but never described in full detail in the literature. Until a series of B-DNA·spermine crystal structures are determined, the mode of action of this important polyamine cannot be fully understood. Finally, it should be noted that polyamines are not the only class of molecules which can induce the B–Z transition very efficiently. A series of Lys-containing peptides with AK repeats, such as KAKAK and KAKAKAK, were recently shown to belong to the class of strongest inducers of the B–Z transition with poly(dG–m^5dC) (Takeuchi et al., 1991). It will be interesting to see whether such peptides exert their effect in a way similar to the intrahelix spermine molecule in the present structure through interactions with functional groups of Z-DNA within and along the minor groove.

ACKNOWLEDGMENT

We thank Dr. Reinhard V. Gessner for helpful discussions and Paolo Lubini for expert assistance with the anisotropic refinement.

REFERENCES

Basu, H. S., & Marton, L. J. (1987) *Biochem. J. 244*, 243–246.
Basu, H. S., Schwietert, H. C. A., Feuerstein, B. G., & Marton, L. J. (1990) *Biochem. J. 269*, 329–334.
Behe, M. J., & Felsenfeld, G. (1981) *Proc. Natl. Acad. Sci. U.S.A. 78*, 1619–1623.
Chen, H. H., Behe, M. J., & Rau, D. C. (1984) *Nucleic Acids Res. 12*, 2381–2389.
Chen, S.-L., & Quigley, G. J. (1992) *Conference Abstracts of the American Crystallographic Association 1992 Annual Meeting/Pittsburgh Diffraction Conference, 50th Annual Meeting*, p 103.
Chevrier, B., Dock, A. C., Hartmann, B., Leng, M., Moras, D., Thuong, M. T., & Westhof, E. (1986) *J. Mol. Biol. 188*, 707–719.
Drew, H. R., Samson, S., & Dickerson, R. E. (1982) *Proc. Natl. Acad. Sci. U.S.A. 79*, 4040–4044.
Egli, M., Williams, L. D., Gao, Q., & Rich, A. (1991) *Biochemistry 30*, 11388–11402.
Eisenstein, M., Hope, H., Haran, T. E., Frolow, F., Shakked, Z., & Rabinovich, D. (1988) *Acta Crystallogr. B44*, 625–628.
Gessner, R. V., Quigley, G. J., Wang, A. H.-J., van der Marel, G. A., van Boom, J. H., & Rich, A. (1985) *Biochemistry 24*, 237–240.
Gessner, R. V., Frederick, C. A., Quigley, G. J., Rich, A., & Wang, A. H.-J. (1989) *J. Biol. Chem. 264*, 7921–7935.
Haworth, I. S., Rodger, A., & Richards, W. G. (1992) *J. Biomol. Struct. Dyn. 10*, 195–211.
Hendrickson, W. A., & Konnert, J. H. (1981) in *Biomolecular Structure, Conformation, Function and Evolution* (Srinivasan, R., Ed.) Vol. I, pp 43–57, Pergamon Press, Oxford.
Ho, P. S., Frederick, C. A., Saal, D., Wang, A. H.-J., & Rich, A. (1987) *J. Biomol. Struct. Dyn. 4*, 521–534.
Hope, H. (1988) *Acta Crystallogr. B44*, 22–26.
Iitaka, Y., & Huse, Y. (1965) *Acta Crystallogr. 18*, 110–121.
Jain, S., Zon, G., & Sundaralingam, M. (1989) *Biochemistry 28*, 2360–2364.
Jones, T. A. (1982) in *Computational Crystallography* (Sayre, D., Ed.) Vol. 11, pp 303–317, Clarendon Press, Oxford.
North, A. C. T., Phillips, D. C., & Matthews, F. S. (1968) *Acta Crystallogr. A24*, 351–359.
Ohishi, H., Kunisawa, S., van der Marel, G. A., van Boom, J. H., Rich, A., Wang, A. H.-J., Tomita, K., & Hakoshima, T. (1991) *FEBS Lett. 284*, 238–244.
Pohl, F. M., & Jovin, T. M. (1972) *J. Mol. Biol. 67*, 375–396.
Quigley, G. J., Teeter, M. M., & Rich, A. (1978) *Proc. Natl. Acad. Sci. U.S.A. 75*, 64–68.
Rao, M. V. R., Atreyi, M., & Saxena, S. (1990) *Biopolymers 29*, 1495–1497.
Schneider, B., Ginell, S. L., Jones, R., Gaffney, B., & Berman, H. M. (1992) *Biochemistry 31*, 9622–9628.
Sheldrick, G. R. (1993) SHELXL-93 crystal structure refinement program, University of Göttingen, Germany.

Takeuchi, H., Hanamura, N., Hayasaka, H., & Harada, I. (1991) *FEBS Lett. 279*, 253–255.
Thomas, T. J., & Messner, R. P. (1986) *Nucleic Acids Res. 14*, 6721–6733.
Thomas, T. J., & Messner, R. P. (1988) *J. Mol. Biol. 201*, 463–467.
Thomas, T. J., Gunnia, U. B., & Thomas, T. (1991) *J. Biol. Chem. 266*, 6137–6141.
Tomita, K., Hakoshima, T., Inubushi, K., Kunisawa, S., Ohishi, H., van der Marel, G. A., van Boom, J. H., Wang, A. H.-J., & Rich, A. (1989) *J. Mol. Graphics 7*, 71–75.
Vertino, P. M., Bergeron, R. J., Cavanaugh, P. F., Jr., & Porter, C. W. (1987) *Biopolymers 26*, 691–703.
Wang, A. H.-J., Quigley, G. J., Kolpak, F. J., Crawford, J. L., van Boom, J. H., van der Marel, G. A., & Rich, A. (1979) *Nature 282*, 680–686.
Wang, A. H.-J., Quigley, G. J., Kolpak, F. J., van der Marel, G. A., van Boom, J. H., & Rich, A. (1981) *Science 211*, 171–176.
Wang, A. H.-J., Hakoshima, T., van der Marel, G. A., van Boom, J. H., & Rich, A. (1984) *Cell 37*, 321–331.
Williams, L. D., Frederick, C. A., Ughetto, G., & Rich, A. (1990) *Nucleic Acids Res. 18*, 5533–5541.